Available online at www.sciencedirect.com

ScienceDirect

Journal of Catalysis 244 (2006) 251–254

JOURNAL OF CATALYSIS

www.elsevier.com/locate/jcat

Research Note

Self-assembly of mesoporous Ni–B amorphous alloy catalysts

Hexing Li [a,*], Qingfei Zhao [a], Ying Wan [a], Weilin Dai [b], Minghua Qiao [b]

[a] *Department of Chemistry, Shanghai Normal University, Shanghai 200234, PR China*
[b] *Department of Chemistry, Fudan University, Shanghai 200433, PR China*

Received 14 July 2006; revised 25 August 2006; accepted 26 August 2006

Abstract

Mesoscopically spherical Ni–B amorphous alloy nanoparticles were prepared through self-assembly of an ionic surfactant hexadecyltrimethyl-ammonium bromide. During liquid-phase nitrobenzene hydrogenation, the as-prepared mesoporous Ni–B catalyst exhibited higher activity and selectivity than the regular Ni–B obtained via direct chemical reduction, apparently owing to the higher surface area, which ensured high dispersion of active sites and the mesoporous channels that might facilitate diffusion and adsorption of reactant molecules.

Keywords: Ni–B amorphous alloy; Mesoporous structure; Surfactant self-assembly; Nitrobenzene hydrogenation

1. Introduction

Amorphous alloy catalysts have been widely studied in past decades owing to their higher activity, better selectivity, and stronger poison resistance in many hydrogenation reactions. Ni–B is perhaps one of the most thoroughly studied of these catalysts [1–5]. Regular Ni–B amorphous alloy catalysts are usually prepared via direct chemical reduction of Ni(II) ions by KBH_4 in aqueous solution. These Ni–B particles are nonporous, with broad size distribution due to agglomeration. Theoretically, depositing Ni–B particles on porous supports could effectively improve the dispersion of Ni–B particles [6–8]. However, due to the weak reducing ability of aqueous KBH_4, only the supported Ni^{2+} ions obtained via impregnation can be completely reduced to Ni–B alloy, which usually results in poor distribution. Recently, mesoporous metals have caused much attention due to their potential application and fundamental interest in catalysis [9–12], but no studies on amorphous alloys have been reported so far. In this paper, we report a novel Ni–B amorphous alloy catalyst with mesoporous structure obtained by chemical reduction in the presence of organic template. Its catalytic performance was examined and compared with regular Ni–B during liquid-phase nitrobenzene hydrogenation. The correlation to the structural characteristics is discussed briefly.

2. Experimental

The mesoporous Ni–B amorphous alloy, denoted meso Ni–B, was prepared based on the self-assembly of hexadecyltrimethyl-ammonium bromide (CTAB). In a typical synthesis, 2.0 g of CTAB dissolved in 15 ml of H_2O was added to a 10 ml $NiCl_2$ aqueous solution containing 0.5 g of Ni at 313 K and was well mixed by stirring for 30 min to ensure self-assembly. After 5 h of aging, 20 ml of a 1.0 M KBH_4 aqueous solution containing 0.20 M NaOH was added dropwise under vigorous stirring at 273 K. After complete reduction of Ni^{2+} ions, the resulting black solid was washed free of inorganic ions and soluble organic substances with distilled H_2O and then transferred into 500 ml of absolute alcohol (EtOH) to extract CTAB by stirring the solution at 353 K for another 10 h. The as-prepared meso Ni–B sample was washed thoroughly with EtOH and finally kept in EtOH until use. The catalysts were characterized by X-ray powder diffraction (XRD), Fourier transform infrared (FTIR), N_2 adsorption–desorption (BET, NOVA 4000e), transmission electron microscopy (TEM), X-ray photoelectron spectroscopy (XPS), H_2 chemisorption, and H_2 temperature-programmed desorption (TPD).

---

[*] Corresponding author.
E-mail address: hexing-li@shnu.edu.cn (H. Li).

0021-9517/$ – see front matter © 2006 Elsevier Inc. All rights reserved.
doi:10.1016/j.jcat.2006.08.025

The nitrobenzene hydrogenation activity test was carried out in a 200 ml autoclave, in which the as-prepared catalyst containing 0.4 g of Ni, 5.0 ml of nitrobenzene, and 30 ml of EtOH were mixed at 363 K and 1.0 MPa H_2 pressure. According to the drop in H_2 pressure with time, the specific activity (R^m (mol/(h g Ni)) and the areal activity (R^S (mol/(h m^2 Ni)) were calculated. The reaction products were analyzed by a gas chromatograph equipped with a flame ionization detector. Reproducibility was checked by repeating the runs at least three times and was found to be within acceptable limits (±5%).

3. Results and discussion

The FTIR spectra demonstrated that the meso Ni–B precursor before EtOH extraction displayed strong absorbance peaks at 2918, 2844, 960, and 910 cm^{-1} corresponding to the ν(C–H), δ(C–H), ν(C–C), and ν(N–H) vibrations in the CTAB molecule, respectively [13]. After being extracted by EtOH, the meso Ni–B sample displayed nearly the same FTIR spectrum as the regular Ni–B obtained via direct chemical reduction in the absence of CTAB. No significant absorbance peaks indicative of the CTAB molecule were observed, indicating that the EtOH extraction could effectively remove the CTAB molecules from the Ni–B amorphous alloy. The absorbance peaks at 1475 and 726 cm^{-1} may be attributed to B_2O_3 species coexisting in the Ni–B amorphous alloy.

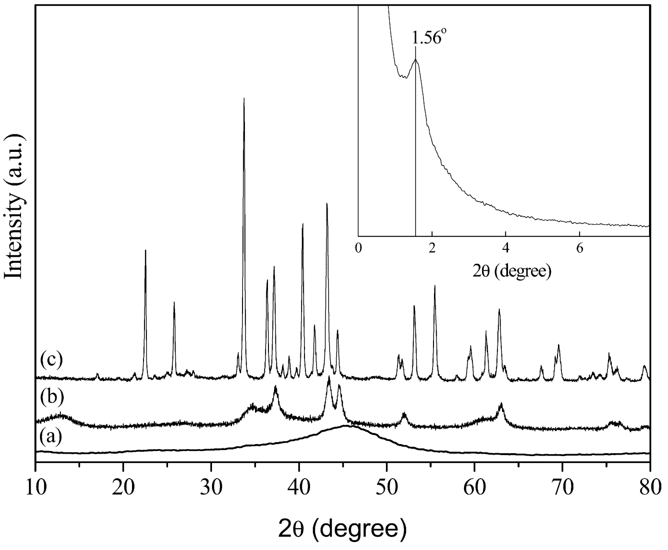

Fig. 1. XRD patterns (a) the fresh meso Ni–B, (b) and (c) the meso Ni–B samples after being treated at 573 K and 873 K in N_2 atmosphere for 2 h, respectively. The inset is the small-angle XRD pattern of the fresh meso Ni–B sample.

As shown in Fig. 1, the XRD patterns demonstrated that the fresh meso Ni–B was present in a typical amorphous alloy structure, because only one broad peak around $2\theta = 45.5°$ was observed [14]. Treatment at elevated temperature resulted in stepwise crystallization of the Ni–B amorphous alloy. The small-angle XRD pattern displayed a well-resolved diffraction peak around $2\theta = 1.56°$, implying the presence of mesoporous structure in the meso Ni–B. This was also confirmed by N_2 the adsorption–desorption isotherm, which displayed a typical IV-type isotherm with H_1 hysteresis [15] and a narrow size distribution centered at 3.8 nm. The weak peak strength and the absence of additional small peaks at higher 2θ compared with the typical mesoporous materials, such as MCM-41 and SBA-15 [16,17], implied poor ordering of the mesoporous structure in the meso Ni–B, as was further confirmed by TEM. Fig. 2 shows that the regular Ni–B is present in nonporous and nearly shapeless particles due to agglomeration, but the meso Ni–B is present in uniform spherical particles of around 120 nm. The worm-like porous structure can be seen from the enlarged TEM image. Such a mesoporous structure could be preserved after the meso Ni–B sample was treated at 473 K for 2 h in N_2 flow. However, further increases in the treating temperature resulted in complete collapse of the mesoporous structure.

The XPS spectra revealed that Ni species in the meso Ni–B sample were present in both the metallic and the oxidized states, corresponding to binding energy (BE) values of 853.1 and 856.6 eV, respectively. Alloyed B and oxidized B species were also detected in the B_{1S} level, corresponding to BE values of 187.9 and 193.2 eV, respectively. In comparison with the standard BE of the pure B (187.1 eV), a positive shift of ca. 0.8 eV was observed, suggesting alloying between Ni and B with partial electron transfer from B to Ni, as found in regular Ni–B amorphous alloy [18]. Much more oxidized Ni and oxidized B species were present in the meso Ni–B than in the regular Ni–B [18], possibly due to the poor reducing ability of KBH_4 in the presence of CTAB surfactant or due to high surface area and thus a higher likelihood of oxidation.

Based on the consideration of surfactant self-assembly, the formation of the worm-like mesoporous meso Ni–B might be as described in Scheme 1. Surfactant self-assembly resulted in a micellar structure that, when concentrated, underwent a second stage of self-assembly and formed liquid-crystalline mesophases. Similar to the self-assembly process of silicate and surfactant [19], Ni^{2+} ions and surfactant could co-assemble and form nanocomposites containing ordered surfactant lyotropic liquid crystalline phases. Chemical reduction of these Ni^{2+} ions by KBH_4 resulted in the formation of the Ni–B amorphous alloy particles surrounding the micellar structure, which com-

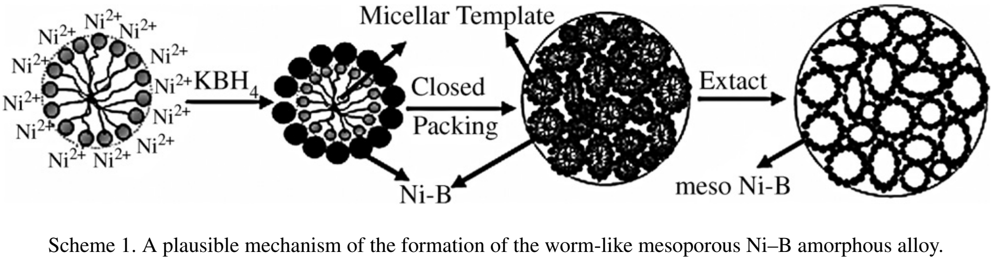

Scheme 1. A plausible mechanism of the formation of the worm-like mesoporous Ni–B amorphous alloy.

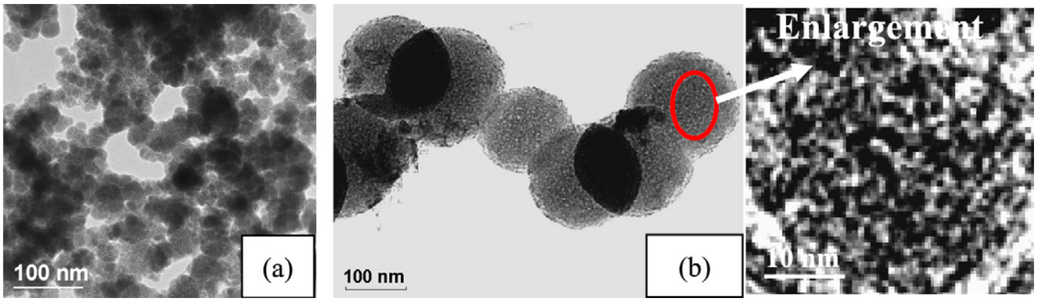

Fig. 2. TEM images of (a) the regular Ni–B and (b) the fresh meso Ni–B samples.

bined into a Ni–B cluster as a wall of the mesopore through metallic bonding and/or –Ni–B–Ni–B– bonding [20]. Many clusters closely packed to form a spherical Ni–B particle. Extraction of the CTAB surfactant by EtOH resulted in the mesoporous structure of each Ni–B particle. Due to the damage of the pore structure of the liquid crystalline surfactant assembly during the close packing and/or extraction, only worm-like pore structure was obtained. The surfactant concentration played a key role in the formation of the mesoporous structure. At very low CTAB concentration (<1.0 g), only the nonporous Ni–B particles were obtained, whereas a very high CTAB concentration (>3.5 g) resulted in a core–shell structure, possibly due to the presence of a large amount of oxidized Ni and B species.

Table 1 shows that both the meso Ni–B and the regular Ni–B had similar compositions, as determined by ICP analysis. However, the meso Ni–B exhibited much higher S_{Ni} than the regular Ni–B, obviously due to the mesoporous structure.

The hydrogenation of nitrobenzene comprises various successive steps. Before the final production of aniline, at least two intermediates might be formed through semihydrogenation [21,22]:

$$C_6H_5\text{–}NO_2 \rightarrow C_6H_5\text{–}NO \rightarrow C_6H_5\text{–}NHOH \rightarrow C_6H_5\text{–}NH_2.$$

Under the present conditions, only aniline was detected during nitrobenzene hydrogenation over the meso Ni–B catalyst, whereas one side product was found when the regular Ni–B catalyst was used. The lower selectivity to aniline over the regular Ni–B (89%) than over the meso Ni–B (100%) could be interpreted in terms of H_2-TPD. As shown in Fig. 3, the meso Ni–B displayed only two TPD peaks concentrated at 557 and 643 K, whereas the regular Ni–B exhibited three TPD peaks located at ca. 476, 613, and 648 K. The lower number of TPD peaks in the meso Ni–B catalyst suggests relatively uniform active sites. The principal TPD peak in the regular Ni–B at around 476 K indicates weak adsorption of hydrogen on the regular Ni–B catalyst. These weakly adsorbed hydrogen atoms are less active than strongly adsorbed hydrogen atoms [21] and thus cannot completely hydrogenate the nitro group to amine.

Comparing the R^{m} values in Table 1 reveals that the meso Ni–B was much more active than the regular Ni–B. One important reason for this is the greater surface area, which ensures high dispersion of the Ni active sites (see the S_{Ni} values listed in Table 1) and the mesoporous channels, which may facilitate diffusion and adsorption of reactant molecules. From the R^{S} values, we can also conclude that the meso Ni–B exhibited a higher intrinsic activity than the regular Ni–B, possibly due to the stronger adsorption of hydrogen on the meso Ni–B (as mentioned above) which might favor hydrogenation of the nitro group.

Table 1
Structural parameters and catalytic properties of the Ni–B samples[a]

Catalyst	Composition (at%)	S_{Ni} (m^2/g Ni)	R^{m} (mmol/(h g Ni))	R^{S} (mmol/(h m^2 Ni))
Meso Ni–B	$Ni_{75.1}B_{24.9}$	31.5	297	9.4
Regular Ni–B	$Ni_{74.5}B_{25.5}$	12.0	82	6.8

[a] Reaction conditions: 0.4 g Ni, 5 ml nitrobenzene, and 30 ml EtOH, $T = 363$ K, $P_{H_2} = 1.0$ MPa, stirring rate = 1000 rpm.

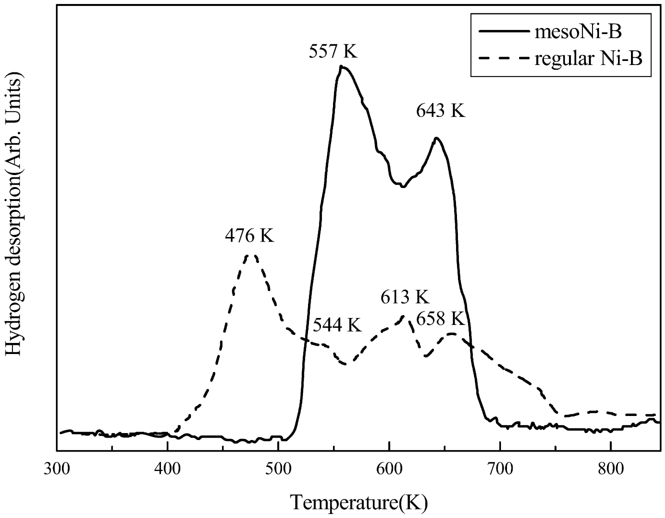

Fig. 3. Hydrogen TPD curves of the fresh meso Ni–B and regular Ni–B samples.

4. Conclusion

Our results illustrate the potential importance of surfactant self-assembly for the preparation of mesoporous amorphous alloys as hydrogenation catalysts. Besides the Ni-based amorphous alloys, other metal-based amorphous alloys, such as Co–B, Ru–B, and Fe–B, could be prepared similarly. These catalysts may exhibit higher activity and even better selectivity than the regular amorphous alloy catalysts because of the higher surface area and the mesoporous structure, as well as the relatively uniform active sites.

Acknowledgments

This work is supported by the National Natural Science Foundation of China (20377031) and the Science and Technology Ministry of China (2005CCA01100).

References

[1] A. Molnar, G.V. Smith, M. Bartok, Adv. Catal. 36 (1989) 329.
[2] Y. Chen, Catal. Today 44 (1998) 3.
[3] H. Li, H.X. Li, J.F. Deng, Mater. Lett. 50 (2001) 41.
[4] H.X. Li, W.J. Wang, J.F. Deng, J. Catal. 191 (2000) 257.
[5] H.X. Li, Y. Wu, H. Luo, M. Wang, Y. Xu, J. Catal. 214 (2003) 15.
[6] H.X. Li, Y. Xu, J.F. Deng, Appl. Catal. 216 (2001) 51.
[7] W.J. Wang, H.X. Li, J.F. Deng, Appl. Catal. 184 (1999) 33.
[8] H.X. Li, W. Wang, J.F. Deng, J. Catal. 194 (2000) 211.
[9] G.S. Attard, N.R.B. Coleman, J.M. Elliot, Stud. Surf. Sci. Catal. 117 (1998) 89.
[10] F. Bouchama, M.B. Thathagar, G. Rothenberg, D.H. Turkenburg, E. Eiser, Langmuir 20 (2004) 477.
[11] G.S. Attard, S.A.A. Leclerc, S. Maniguet, A.E. Russell, I. Nandhakumar, P.N. Bartlett, Chem. Mater. 13 (2001) 1444.
[12] G.S. Attard, S.A.A. Leclerc, S. Maniguet, A.E. Russell, I. Nandhakumar, B.R. Gollas, P.N. Bartlett, Microporous Mesoporous Mater. 44 (2001) 159.
[13] A.S.M. Chong, X.S. Zhao, J. Phys. Chem. B 107 (2003) 12650.
[14] H. Yamashita, M. Yoshikawa, T. Funabiki, S. Yoshida, J. Chem. Soc. Faraday Trans. I 82 (1986) 1771.
[15] Y. Lu, H. Fan, A. Stump, T.L. Ward, T. Rieker, C.J. Brinker, Nature 398 (1999) 223.
[16] D. Zhao, J. Feng, Q. Huo, N. Melosh, G.H. Fredrickson, B.F. Chemelka, G.D. Stucky, Science 279 (1998) 548.
[17] X. Wang, K.S. Lin, J.C. Chan, S. Cheng, Chem. Commun. (2004) 2762.
[18] H. Li, H.X. Li, W. Dai, J.F. Deng, Appl. Surf. Sci. 152 (1999) 25.
[19] D.W. Schaefer, MRS Bull. 19 (1994) 14.
[20] B. Shen, S. Wei, K. Fan, J.F. Deng, Appl. Phys. A 65 (1997) 295.
[21] A.M. Stratz, Chem. Ind. 18 (1984) 335.
[22] F. Pinna, M. Signoretto, G. Strukul, J. Catal. 150 (1994) 36.